Molecular Dynamics Study of the Complexation Mechanism of Functional Groups with Copper Formate

1st Li Liu
School of Materials Science and Engineering
Wuhan University of Technology
Wuhan, China
liuli.whut@outlook.com

2nd Haojie Ma
School of Materials Science and Engineering
Wuhan University of Technology
Wuhan, China
hma818149@outlook.com

3rd Yuan Yuan
School of Materials Science and Engineering
Wuhan University of Technology
Wuhan, China
15271289370@163.com

4th Xianglong Jia
School of Materials Science and Engineering
Wuhan University of Technology
Wuhan, China
281047@whut.edu.cn

5th Willem D. van Driel
Department of Microelectronics
Delft University of Technology
Delft, Netherlands
willem.vandriel@tudelft.nl

6th Guoqi Zhang
Department of Microelectronics
Delft University of Technology
Delft, Netherlands
g.q.zhang@tudelft.nl

7th Zhiwen Chen*
The institute of Technological Science
Wuhan University
Wuhan, China
zwchen_lu@163.com

2025 26th International Conference on Electronic Packaging Technology (ICEPT) | 978-1-6654-6580-9/25/$31.00 ©2025 IEEE | DOI: 10.1109/ICEPT67137.2025.11157510

***Abstract*—Flexible printed electronics (FPE) technology has a broad application prospect due to their low cost and energy consumption. Copper-based nanoinks have emerged as viable substitutes for precious metals owing to their excellent electrical conductivity and affordability. However, their tendency toward oxidative agglomeration remains a challenge, which requires to be optimized through strategies like low-temperature sintering and metal-organic decomposition (MOD). In this study, copper formate was selected as the precursor, and four complexing agents including 2-amino-2-methyl-1-propanol (AMP), 2-amino-2-methyl-1,3-propanediol (AMPD), isopropanol (IPA), and isopropylamine were evaluated, respectively. Molecular dynamics (MD) simulations were employed to investigate how different functional groups (-NH_2, -OH, -CH_3) influence the coordination mechanism with Cu^{2+} ions. The results show that Cu^{2+} mainly coordinated with hydroxyl and amine groups. Among the four complexing agent systems, the IPA system had the most complete complexation decomposition, produced the most gases (~ 57%) and the least organic residues (~16.26%), and showed to be the most suitable for the configuration of copper inks.**

Keywords—copper formate complexes; molecular dynamics; functional group interactions

I. Introduction

In recent years, as several fields including flexible electrodes, solar cells, and sensors are increasingly moving toward scalable and low-cost manufacturing, traditional processes like photolithography, etching, and electroplating are being gradually replaced by emerging techniques such as Flexible Printed Electronics (FPE) [1]. FPE is a simple, fast, and cost-effective additive manufacturing method that enables the printing of nanoparticle (NP) inks onto flexible substrates to fabricate high-resolution devices [2-3].

Metal nanoparticles, especially for gold and silver, have been widely used in printed electronic inks due to their excellent electrical conductivity [4-5]. Nevertheless, the high cost of these precious metals significantly limits their wide application. In contrast, copper-based NP inks offers a promising low-cost alternative while maintaining excellent electrical properties [6]. However, copper nanoparticles are prone to oxidation and agglomeration, which hinders their practical application. Therefore, enormous researches have been conducted to propose various low-temperature sintering strategies for overcoming these above challenges [7].

Copper-based Metal-Organic Decomposition (MOD) inks, free of copper particles, form nanoparticles via low-temperature decomposition, can effectively mitigate agglomeration and sedimentation issues [8-10]. The core mechanism lies in this process is the complexation between copper ions and organic ligands. Zhang *et al.* [11] developed an MOD ink using an isooctylamine/AMP coordination system and 0.25 wt.% Cu-CNTs, achieving 30×10^{-5} Ω·cm resistivity just in air. Samani *et al.* [12] optimized a copper acetate/AMP (1:2) system, attaining 30 μΩ·cm resistivity at 180°C under N_2. Li *et al.* [13] synthesized a 36.8% metal-loaded oxidation-resistant copper film via copper tetrahydrate formate/AMP at 140°C in nitrogen atmosphere, demonstrating superior surface morphology and stability. Despite these advancements, the unclear complexation mechanisms between copper precursors and organics hinder further optimization of MOD ink performance. Thus, a comprehensive study on how different functional groups (e.g., -NH_2, -OH, and -CH_3) influence the coordination with Cu^{2+} ions is essential for improving the performance of copper ink. Current experimental methods are not only costly and time consuming, but also limited in their ability to reveal the underlying mechanisms of bond dissociation and formation. Molecular dynamics (MD)

simulations offer a powerful approach to study the complexation interactions at the atomic level.

In this work, copper formate was selected as the precursor, and four complexing agents including 2-amino-2-methyl-1-propanol (AMP), 2-amino-2-methyl-1,3-propanediol (AMPD), isopropanol (IPA), and isopropylamine were investigated. The aim of this work was to study and compare how different functional groups (-NH_2, -OH and -CH_3) affect their coordination behaviors with Cu^{2+} ions. The results are expected to provide theoretical insights into the stability of copper formate complexes and to support the formulation design of high-performance MOD inks.

II. Methodology

As illustrated in Figure 1, the MD models were constructed using the Packmol program and simulated in the Large-scale Atomic Molecular Massively Parallel Simulator (LAMMPS). Periodic boundary conditions were applied in all three spatial directions (x, y, and z). The ReaxFF potential function was employed to accurately capture bond formation and breaking processes [14].

Before the start of simulation, energy minimization was performed using the conjugate gradient algorithm, followed by a 10 ps relaxation at 200k within the NVT ensemble to ensure system stability and avoid excess internal energy. The subsequent MD simulation was conducted in the NVE ensemble at 1273.15k for 500 ps, with temperature control provided by the Berendson thermostat. Simulation outputs were then analyzed and visualized [15]. The detailed simulation parameters are listed in Table 1.

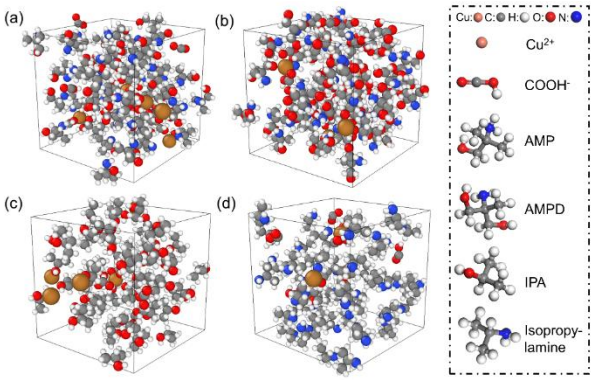

Figure 1 MD models of copper formate complexation with (a) AMP, (b) AMPD, (c) IPA, (d) Isopropylamine.

Table 1 Detailed simulation parameters.

System	Complexing agent structure	Volume of box(Å^3)	Temperature (K)	Simulation time(ps)
5 $Cu(COOH)_2$ 50 $C_4H_{10}NO$	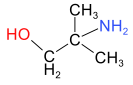	21.0*21.0 *21.0	1273.15	500
5 $Cu(COOH)_2$ 50 $C_4H_{11}NO$	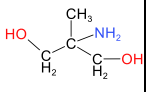	20.8*20.8 *20.8	1273.15	500
5 $Cu(COOH)_2$ 50 C_3H_8O	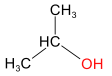	19.9*19.9 *19.9	1273.15	500
5 $Cu(COOH)_2$ 50 C_3H_9N	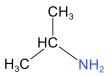	20.7*20.7 *20.7	1273.15	500

III. Results and Duscussion

A. RDF Analysis

The radial distribution function (RDF) is an important physical quantity used to describe the atomic-scale structure of materials. It characterizes the probability of finding a specific type of atom B at a distance r from a reference atom A, thereby offering insight into atomic arrangement and local ordering. The RDF is defined by Equation (1).

$$g_{AB}(r) = \frac{n_B(r)}{\rho_B \cdot V_{\text{shell}}} = \frac{n_B(r)}{\left(\frac{N_B}{V}\right) \cdot 4\pi r^2 \, \Delta r} \qquad (1)$$

Where $n_B(r)$ is the number of B atoms located within a spherical shell of thickness Δr around the reference atom A. N_B is the total number of B atoms in the system. V is the total system volume, and V_{shell} represents the volume of the spherical shell at distance r. For well-ordered atomic systems, the RDF value typically rises rapidly to a peak and then decays towards 1, showing structural stability and homogeneity.

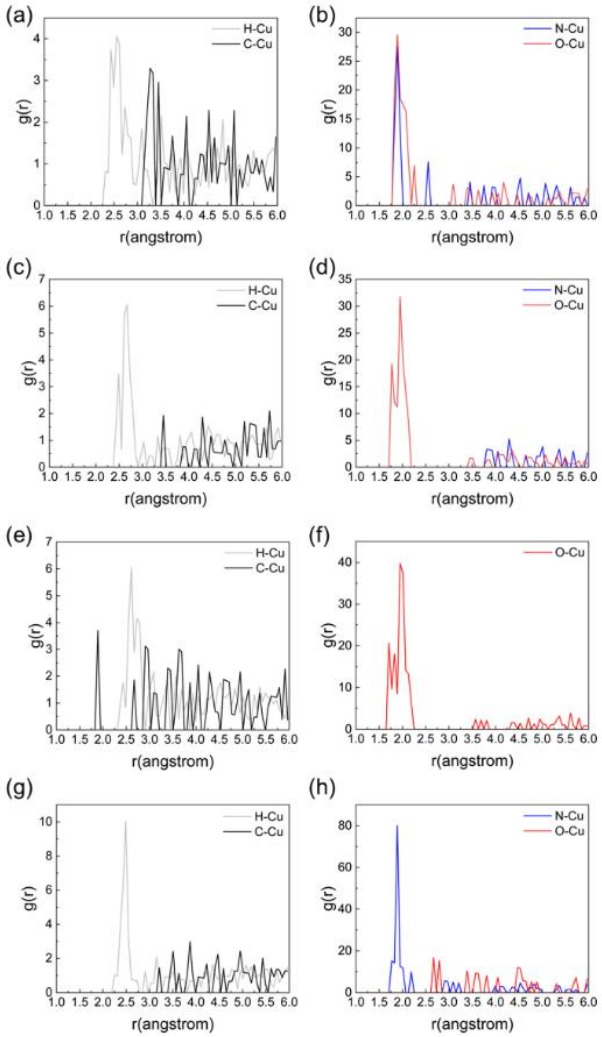

Figure 2 Radial distribution functions (RDFs) of (a)(b) AMP, (c)(d) AMPD, (e)(f) IPA, and (g)(h) isopropylamine systems.

Figure 2 presents the RDFs between Cu atoms and C, N, H, and O atoms in the four complexation systems involving AMP, AMPD, IPA, and isopropylamine. The height of each RDF peak indicates the local density of neighboring atoms and provides qualitative information about bond compactness

and interaction strength [16]. Notably, the results clearly show that Cu-O and Cu-N interactions are significantly stronger than those with H or C atoms, indicating that hydroxyl and amine groups are the dominant ligands coordinating with Cu^{2+} ions. In addition, the average bond lengths between Cu and its nearest neighbors can be inferred from the position of the first RDF peak [17], with shorter bond distances typically corresponding to higher dissociation energies [18].

In the AMP complex, the Cu-N and Cu-O bond lengths are both approximately 1.9 Å, indicating similar coordination strength. In contrast, the AMPD complex exhibits a shorter Cu-O bond (~1.8 Å) compared to its Cu-N bond, suggesting that coordination with the hydroxyl group is stronger in this system. For the isopropylamine complex, a shorter Cu–N bond indicated enhanced Cu–N interactions. Consistment with the presence of a single amine group.

B. Overall products analysis

Figure 3 demonstrates the evolution of both molecular and species populations during the complexation process across the four systems. In the AMP system (see Fig. 3a), the number of molecules and species increased significantly over time, indicating a high active complexation reaction. As shown in Fig. 3b, in the AMPD system, the number of species rose rapidly at the initial stage and then plateaued, suggesting a fast reaction rate but limited products density. In contrast, although the total numbers of molecules in the IPA (see Fig. 3c) and isopropylamine (see Fig. 3d) systems were higher, the number of distinct species increased more slowly and remained relatively low. This indicates that most molecules in these systems remained either unreacted or formed simple, less diverse complexes.

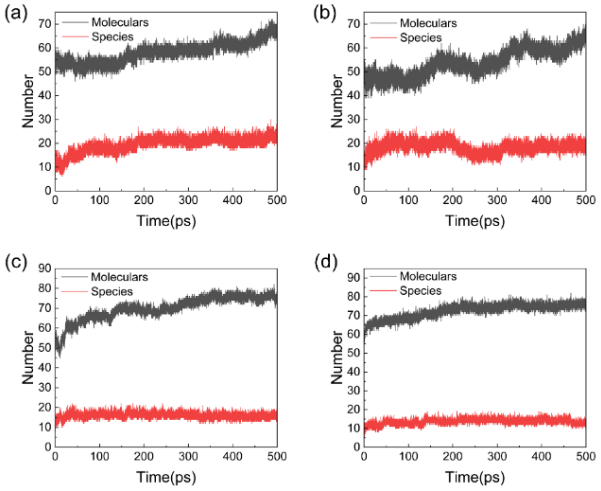

Figure 3 Evolution of molecular and species populations during the complexation of copper formate with (a) AMP, (b) AMPD, (c) IPA, and (d) isopropylamine.

Figure 4 presents the product distribution at 100, 300, and 500 ps for each system. All four systems exhibited a gradual increase in gaseous products and a decrease in copper-containing complexes over time. This indicates an ongoing decomposition of organic compounds. The percentage of copper complexes varied little during the reaction of AMP (see Fig.4a), IPA (see Fig.4c) and isopropylamine (see Fig.4d) systems, within 5%. However, after the completion of the reaction of the AMPD system, the percentage of copper complexes decreased by 15% compared with that at 100 ps, as shown in Fig.4b. Furthermore, the content of organic residues decreased by approximately 10-20% in the remaining three systems and increased by about 15% in the AMPD system. This shows that the organic macromolecules generated within the AMPD system are more thermally stable. This enhanced stability is likely due to the presence of multiple hydroxyl groups in AMPD, which act as hydrogen bond donors and form intramolecular hydrogen bonds with amino groups. Such hydrogen bonding networks improve the structural integrity of organic molecules [19].

Upon completion of the reaction, the IPA system had the highest gas content of 57 % and the lowest organic residue of 16.26%. Isopropylamine had the second highest gas content of 40 %. These results align with the increasing number of molecule species observed in both systems as shown in Figure 3. In contrast, the AMP and AMPD systems produced significantly less gas, which is approximately 20%, highlighting their superior thermal stability. Notably, the AMPD system retained the highest level of organic residue at 55.60%. This further supports the proposed decomposition inhibition mechanism by hydrogen bonding networks in complexed systems.

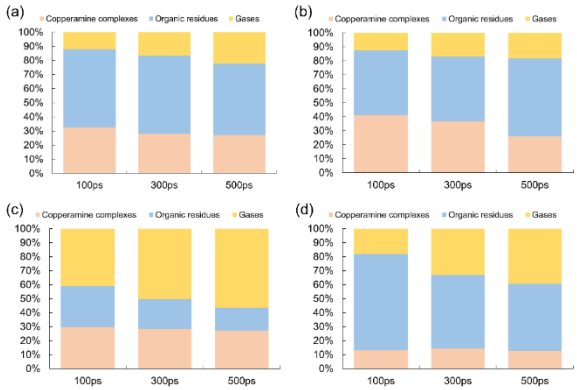

Figure 4 Identified product species at 100 ps, 300 ps, and 500 ps in four systems: (a) AMP, (b) AMPD, (c) IPA, (d) isopropylamine.

C. Gas Mechanism Analysis

Gaseous products can significantly affect the conductivity and quality of copper inks, so the analysis of gas generation mechanisms during complexation is crucial.

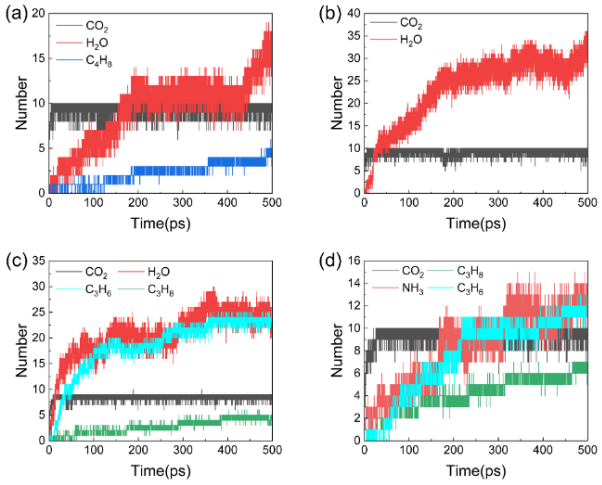

Figure 5 Concentration profiles of major gaseous products during the complexation of copper formate with (a) AMP, (b) AMPD, (c) IPA, and (d) isopropylamine.

Figure 5 presents the concentration profiles of major gaseous species in the AMP, AMPD, IPA, and isopropylamine systems. The primary gas products mainly consisted of CO_2, H_2O (in the vapor phase) and various organic compounds. For simplicity, all water vapor is referred to as H_2O in the following discussion.

In all systems, CO_2 generation was most intense during the first 10 ps of simulation and subsequently reached a dynamic equilibrium as the reactions progressed. The specific formation pathways of these gases are further examined in Fig. 6 to Fig. 9. Notably, systems containing hydroxyl-functionalized ligands (AMP, AMPD, and IPA) exhibited sharp increases in H_2O generation, indicating that hydroxyl groups played a dominant role in promoting water formation.

In contrast, the IPA and isopropylamine systems showed poorer organic stability, likely due to their simpler molecular structures and the presence of only one functional ligand per molecule [20]. The mechanisms underlying the formation of major gas products were then investigated for each system. Figure 6 shows the reaction pathways leading to the generation of CO_2, H_2O, and C_4H_8 in the AMP system. As illustrated in Figure 6a, CO_2 is primarily produced via decarboxylation of carboxylate ions, decomposition and recombination of intermediate species, and the dissociation of –O–Cu–OH complexes. Interestingly, CO_2 can also re-enter the reaction system as a reactant, contributing to a dynamic equilibrium among multiple reaction routes.

H_2O (see Figure 6b) was primarily generated through the direct reaction between AMP and Cu–OH complexes. However, it also participated in subsequent reactions, with the rates of formation and consumption being nearly balanced. This dynamic explains the increasing H_2O concentration observed in Figure 5a, which is mainly attributed to the activation and rearrangement of carboxylic acid groups. In addition, C_4H_8 (see Figure 6c) was mainly formed through sequential dehydroxylation and amination of AMP. These results indicate that although the coordination strengths of hydroxyl and amino groups with Cu^{2+} were found to be comparable in the AMP system as shown in Figure 2, copper ions exhibited a preference for binding with hydroxyl groups.

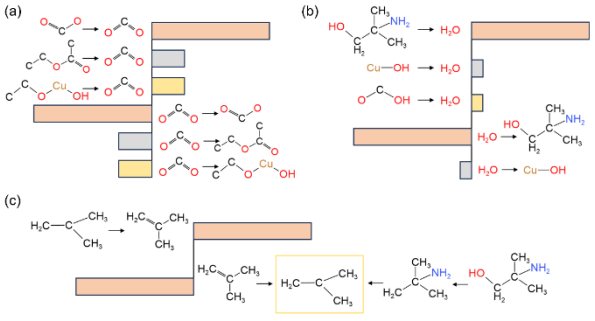

Figure 6 Reaction mechanisms of major gas products in the AMP complex system: (a) CO_2, (b) H_2O, (c) C_4H_8.

In the AMPD system, the primary gaseous products were H_2O and CO_2. As shown in Figure 7a, CO_2 formation followed a mechanism similar to that of AMP and was mainly derived from carboxylate ions. As illustrated in Fig 7b, H_2O was generated primarily from AMPD itself and from intermediates produced after partial dehydroxylation. A smaller contribution came from reactions involving HO–Cu–OH complexes. Similar to the AMP system, Cu^{2+} ions preferentially coordinated with hydroxyl groups.

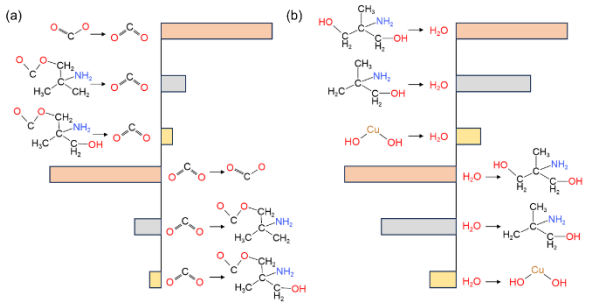

Figure 7 Reaction mechanisms of major gas products in the AMPD complex system: (a) CO_2, (b) H_2O.

The reaction mechanisms for CO_2, H_2O, C_3H_6, and C_3H_8 in the IPA system are illustrated in Figure 8. CO_2 was primarily produced through the decarboxylation of carboxylate ions and recombination reactions involving IPA as shown in Figure 8a, while H_2O (see Figure 8b) was mainly formed via reactions between IPA and the amino group within the Cu–OH complex. Furthermore, dehydroxylation products of IPA served as precursors for the formation of C_3H_6 and C_3H_8 as presented in Fig. 8c and 8d.

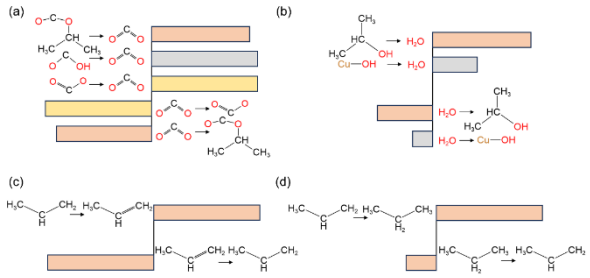

Figure 8 Reaction mechanisms of major gas products in the IPA complex system: (a) CO_2, (b) H_2O, (c) C_3H_6, (d) C_3H_8.

In the isopropylamine system, the primary gases generated were CO_2, NH_3, C_3H_8, and C_3H_6, as shown in Figure 9. Unlike the IPA system, H_2O was not a major product due to the absence of hydroxyl groups and the presence of only one amino group in isopropylamine. This further supports the conclusion that hydroxyl groups play a key role in water generation, as seen in the AMP, AMPD, and IPA systems (see Figures 5 to 8). CO_2 in this system was mainly formed via the rearrangement and decarboxylation of carboxylates following isopropylamine deamination. The production of organic gases was also largely attributed to decomposition reactions after deamination.

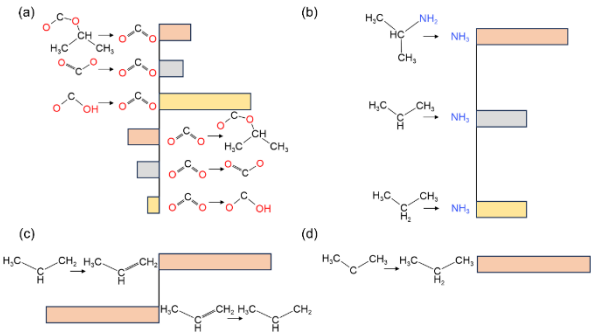

Figure 9 Reaction mechanisms of major gaseous products in the isopropylamine complex system: (a) CO_2, (b) NH_3, (c) C_3H_6, (d) C_3H_8.

Based on the above analyses, gas generation in all four systems can be primarily attributed to the decomposition of carboxylate ions and the interactions with complexing agents. CO_2 was produced through carboxylate decarboxylation, recombination of decomposition products, and ligand dissociation from Cu complexes. H_2O was mainly formed via activation and rearrangement of carboxylic acid groups, reactions involving complexing agents and their intermediates, and the breakdown of copper–ligand complexes. Organic gases were primarily generated from the degradation of intermediates following ligand fragmentation. Notably, in systems containing only a single amino group in the ligand, NH_3 was formed as a distinctive by-product.

D. Complexation mechanism

Following the analysis of overall gas evolution pathways, we now focus on the complexation mechanism between Cu^{2+} and the four selected complexing agents of the AMP, AMPD, IPA, and isopropylamine. The chemical nature and functional groups of these complexing agents plays a vital role in determining the coordination environment of Cu^{2+}, which in turn influences the thermal behavior and performance of MOD inks.

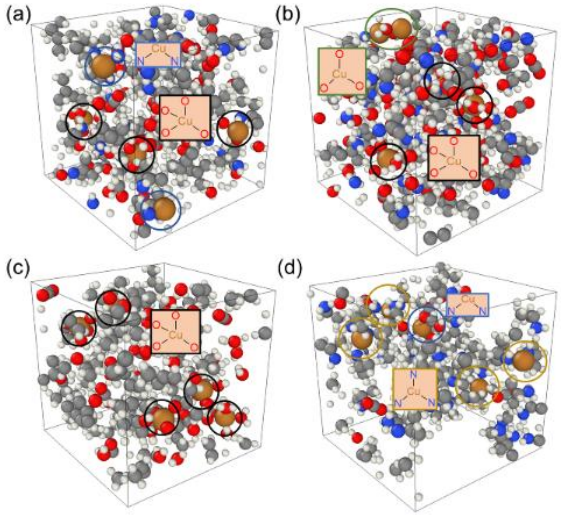

Figure 10 The coordination configurations of copper complexes after 500 ps of MD simulation: (a) AMP, (b) AMPD, (c) IPA, (d) isopropylamine.

As shown in Figure 10, the coordination environments observed after 500 ps of simulation are consistent with the trends revealed by the RDF and gas evolution analysis (see Figure 2 and 6-9). In the AMP system, Cu^{2+} simultaneously coordinate with hydroxyl oxygens and amino nitrogen atoms from multiple AMP molecules. Up to four Cu-O bonds are formed, forming a tetrahedral coordination structure dominated by oxygen. Meanwhile, the nitrogen in the amino group also participated in the coordination to form a Cu-N bond. Although both -OH and $-NH_2$ groups serve as electron donors, Cu^{2+} shows a stronger preference for hydroxyl coordination.

In the AMPD system, a polydentate coordination mode is observed, with Cu^{2+} predominantly forming bonds with hydroxyl groups. The higher number of -OH groups lead to stronger Cu-O interactions. While amino donors are also present but their role is secondary.

In the IPA systems, coordination is exclusively Cu-O, as IPA contains only one hydroxyl group and lacks nitrogen-based donors. Conversely, in the isopropylamine system, Cu-N coordination dominates due to the high nitrogen content. Although some hydroxyl groups generated from carboxylate ions may exist in the system, Cu-N bonding becomes the dominant coordination type due to the density concentration of N in isopropylamine.

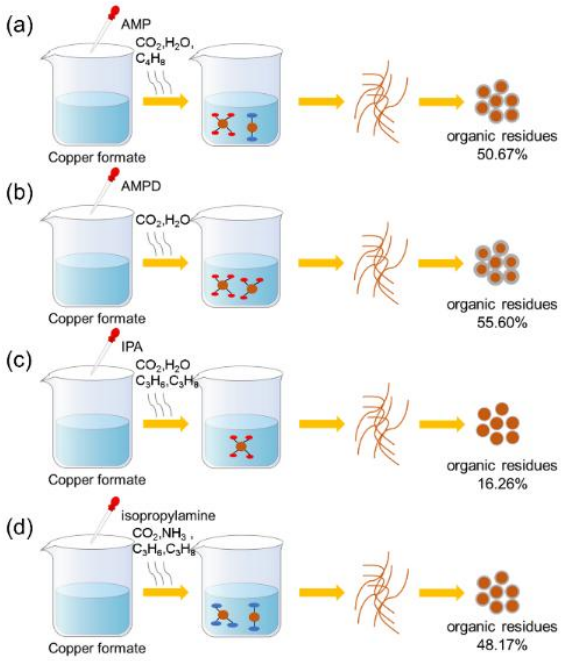

Figure 11 Schematic illustration of the complexation process: (a) AMP, (b) AMPD, (c) IPA, (d) isopropylamine.

Figure 11 presents schematic representations of the complexation process in each system. In the AMP system, Cu^{2+} forms multidentate coordination complexes with both hydroxyl oxygens and amino nitrogens. The presence of a hydrogen bonding network stabilizes the structure, resulting in a high organic residue of 50.67% after complexation. In the AMPD system, which has a greater number of hydroxyl groups, stronger hydrogen bonding, and a stable Cu-$(O)_4$ coordination structure are observed. This leads to the highest organic residue (55.60 %) and enhanced thermal stability.

In contrast, the IPA system lacks hydrogen-bond networks and contains only hydroxyl group, exhibiting the most complete decomposition with a low organic residue of only 16.26%. Although isopropylamine and IPA are structurally similar, the presence of amino groups in the isopropylamine system enables limited hydrogen bonding network, resulting in a higher organic residue of 48.17%.

Taken together, these results demonstrate that the structure and donor atoms of complexing agents directly influence the coordination mode and thermal decomposition behavior of Cu^{2+} complexes. Ligands with multiple functional groups, such as hydroxyl and amino, tend to form stable multidentate complexes, enhancing thermal stability and increasing organic residue. In contrast, ligands with single hydroxyl group favor more complete decomposition and reduced residue. These findings highlight the importance of rational ligand design in regulating the pyrolytic characteristics and optimizing the performance of MOD-based materials.

IV. Conclusion

In this study, the complexation mechanisms of four copper-based MOD ink systems were systematically investigated using MD simulations. For the first time, the dynamic coordination competition behavior of functional groups (-NH_2, -OH, -CH_3) with Cu^{2+} was quantitatively analyzed, providing a theoretical foundation for the rational design of copper-based conductive inks. The key findings are summarized as follows:

1. Hydroxyl and amine groups are the primary ligands coordinating with Cu^{2+}. In the AMP system, the coordination strengths of -OH and -NH_2 groups are comparable due to their equal abundance. In contrast, the additional hydroxyl group in AMPD enhances Cu-O coordination, resulting in a stronger affinity for hydroxyl ligands than amine ligands.

2. The coexistence of hydrogen bonding networks between hydroxyl and amino groups, along with the inherent complexity of the ligands, contribute to the structural stabilization of organic residues. Due to the presence of only hydroxyl groups and a simple molecular structure, the IPA system has the most complete decomposition and the lowest organic residues of 16.26%. Compared to AMP, AMPD and isopropylamine, IPA demonstrates the highest suitability for use in copper conductive ink formulations.

3. Among all systems, CO_2 is primarily generated through carboxylate decarboxylation and Cu-ligand dissociation. H_2O formation mainly arises from the reorganization of carboxylic acid groups and ligand degradation. Organic gases are formed from the breakdown of intermediate species, while NH_3 generation occurs exclusively in systems containing a single amine group.

Acknowledgment

This work was funded by the Marie Skłodowska-Curie Actions Postdoctoral Fellowship (No. 101204306), Major Project of Hubei Province (Functional coating and materials, No. 2023BAA003), National Natural Science Foundation of China (No. 62274122), National Key Research and Development Program of China (No. 2022YFB3207100), Wuhan Knowledge Innovation Special Dawn Program (No. 2023010201020320), and the Natural Science Foundation of Hubei Province for Distinguished Young Scholars (No. 2024AFA064).

References

[1] N. Mohan, J. I. Ahuir-Torres, H. R. Kotadia, and G. Elger, “Laser sintering of Cu particle-free inks for high-performance printed electronics,” npj Flex. Electron., vol. 9, Art. no. 18, Mar. 2025.

[2] Y.-L. Zhou, W.-N. Cheng, Y.-Z. Bai, C. Hou, K. Li, and Y.-A. Huang, "Rise of flexible high-temperature electronics," *Rare Met.*, vol. 42, pp. 1773–1777, 2023.

[3] M. Konar, E. T. Him, N. Guler, E. N. Balci, and N. Arsu, “In situ photochemical synthesis of environmentally friendly conductive nano-ink,” Macromol. Chem. Phys., 2024.

[4] W. Li, Q. Sun, L. Li, J. Jiu, X.-Y. Liu, M. Kanehara, T. Minari, and K. Suganuma, “The rise of conductive copper inks: challenges and perspectives,” National Institute for Materials Science, vol. 18, Art. no. 100451, 2020.

[5] P. Zhang, Q. Sun, S. Fang, et al., “Fabrication of nano copper highly conductive and flexible printed electronics by direct ink writing,” ACS Appl. Mater. Interfaces, vol. 17, p. 1860, 2024.

[6] N. Mohan, J. I. Ahuir-Torres, S. K. Bhogaraju, et al., “Decomposition mechanism and morphological evolution of in-situ realized Cu nanoparticles in Cu complex inks,” *New J. Chem.*, vol. 48, pp. 6796–6808, 2024.

[7] W. Li, L. Li, Y. Gao, et al., “Highly conductive copper films based on submicron copper particles/copper complex inks for printed electronics: Microstructure, resistivity, oxidation resistance, and long-term stability,” J. Alloys Compd., vol. 732, pp. 240–247, 2018.

[8] Y. Wang, D. Xu, H. Yan, et al., “Low-temperature copper sinter-joining technology for power electronics packaging: A review,” J. Mater. Process. Technol., vol. 332, Art. no. 118526, 2024.

[9] W. Qi, R. Han, H. Quan, et al., “Self-reducing molecular ink for printed electronics and lithium-ion battery cathodes as conductive binder,” J. Mater. Chem. C, vol. 12, pp. 5114–5121, 2024.

[10] K. Li and X. Jiang, “The synthesis of copper nanoparticles for printed electronic materials using liquid phase reduction method,” Materials, vol. 17, Art. no. 3069, 2024.

[11] L. Zhang, K. Yang, D. Xue, and S. Zhou, "Improving the performance of copper-based metal-organic decomposition inks modified with copper-coated carbon nanotubes," ChemistrySelect, vol. 10, p. e202405161, 2025.

[12] H. Naderi-Samani et al., "The effects of complex agent and sintering temperature on conductive copper complex paste," *Heliyon*, vol. 8, no. 12, p. e12624, 2022.

[13] W. Li, S. Cong, J. Jiu, S. Nagaoa, and K. Suganumaa, "Self-reducible copper inks composed of copper–amino complexes and preset submicron copper seeds for thick conductive patterns on a flexible substrate," J. Mater. Chem. C, vol. 4, no. 37, pp. 8802–8809, 2016.

[14] J. Yeon, H. L. Adams, C. E. Junkermeier, et al., “Development of a ReaxFF force field for Cu/S/C/H and reactive MD simulations of methyl thiolate decomposition on Cu (100),” J. Phys. Chem. B, vol. 122, no. 2, pp. 888–896, 2017.

[15] Y.-G. Tong, N. Tian, H.-F. Huang, Z.-B. Zhang, X.-B. Liang, X.-X. Ji, J.-Z. Fang, and Y.-L. Hu, "Microstructure and deformation mechanism of dual-phase $Al_{0.5}$CoCrNiFe high-entropy alloy," *Rare Met.*, vol. 42, pp. 2020–2027, 2023.

[16] Z. Wang, X. Li, L. Yu, and J. Song, “Molecular dynamics simulation of effect of carbon nanotube diameter on properties of crosslinked epichlorohydrin rubbers,” Polymers (Basel), vol. 16, no. 17, Art. no. 2419, Aug. 2024.

[17] R. Gómez-Villarejo, E. I. Martín, J. Navas, A. Sánchez-Coronilla, T. Aguilar, J. J. Gallardo, R. Alcántara, D. De los Santos, I. Carrillo-Berdugo, and C. Fernández-Lorenzo, “Ag-based nanofluidic system to enhance heat transfer fluids for concentrating solar power: Nano-level insights,” Appl. Energy, vol. 194, pp. 19–29, May 2017.

[18] M. Kaupp, D. Danovich, and S. Shaik, “Chemistry is about energy and its changes: A critique of bond-length/bond-strength correlations,” Coord. Chem. Rev., vol. 344, pp. 355–362, Aug. 2017.

[19] Y. Ogawa, P.-K. Naito, and Y. Nishiyama, “Hydrogen-bonding network in anhydrous chitosan from neutron crystallography and periodic density functional theory calculations,” Carbohydr. Polym., vol. 207, pp. 211–217, Mar. 2019.

[20] L. Liu, H. Ma, C. Chen, Z. Xu, L. Nong, Y. Zou, X. Xu, X. Wang, and Z. Chen, “Decomposition and sintering behaviors of MOD-assisted Ag pastes for power electronics,” Mater. Today Commun., vol. 45, Art. no. 112265, Apr. 2025.